❒ 1447

Glioma segmentation using hybrid filter and modified African vulture optimization

Bhagyalaxmi Kuntiyellannagari[1], Bhoopalan Dwarakanath[2]
[1]Department of Computer Science and Engineering, Faculty of Engineering and Technology, SRM Institute of Science and Technology, Ramapuram, Chennai, India
[2]Department of Information Technology, Faculty of Engineering and Technology, SRM Institute of Science and Technology, Ramapuram, Chennai, India

Article Info

ABSTRACT

Accurate brain tumor segmentation is essential for managing gliomas, which arise from brain and spinal cord support cells. Traditional image processing and machine learning methods have improved tumor segmentation but are often limited by accuracy and noise handling. Recent advances in deep learning, particularly using U-Net and its variants, have achieved significant progress but still face challenges with heterogeneous data and real-time processing. This study introduces a hybrid bilateral mean filter for noise reduction coupled with an ensemble deep learning model that integrates U-Net, InceptionV2, InceptionResNetV2, and W-Net to enhance segmentation accuracy and efficiency. Additionally, we propose a novel modified African vulture optimization algorithm (MAVOA) to further refine segmentation performance. Evaluated on the BraTS 2020 dataset, our model achieved a loss of 0.023 with strong performance metrics: 98.2% accuracy, 97.2% mean intersection over union (IOU), and 99.1% precision. It effectively segmented glioma subregions with dice scores of 0.96 for necrotic areas, 0.97 for edema, and 0.91 for enhancing regions. On the BraTS 2021 dataset, the model maintained high accuracy 96.4%, mean IOU 95.9%, and dice coefficients of 0.91 for necrotic areas, 0.95 for edema, and 0.92 for enhancing regions.

Corresponding Author:

Bhagyalaxmi Kuntiyellannagari
Department of Computer Science and Engineering, Faculty of Engineering and Technology
SRM Institute of Science and Technology
Ramapuram, Chennai, India
Email: bk8019@srmist.edu.in

1. INTRODUCTION

Glioblastoma is the most common and aggressive type of primary brain tumor. Statistics reveal that 85-90% of all primary central nervous system (CNS) tumors are brain tumors. Newly diagnosed cases of brain and CNS cancer are responsible for about 3% of all cancers globally. In European countries, these cases are five times higher than in Asian countries. Early-stage diagnosis and treatment require automatic segmentation of brain tumors, which is expensive and time-consuming if done manually. Recent advancements in image processing and computer vision have significantly contributed to this area.

Gliomas, a type of brain tumor, are categorized into low-grade glioma (LGG), which grows slowly, and high-grade glioma (HGG), which can be life-threatening. According to the World Health Organization, HGG tumors are critical, with a maximum survival rate of two years, while LGG-affected patients can have several years of life expectancy [1]. Despite advancements in imaging, radiotherapy, and surgical techniques,

some tumors remain untreatable. Among various imaging techniques, magnetic resonance imaging (MRI) is preferred for brain tumor diagnosis due to its ability to produce detailed and clear images compared to computed tomography (CT) scans [2]. Brain tumors typically have three regions: necrotic and non-enhancing tumor, peritumoral edema, and enhancing tumor [3]. Recent advancements in medical imaging and machine learning have improved brain tumor segmentation by enhancing diagnostic accuracy and reducing analysis timecompared to manual methods [4]. Deep learning models, such as U-Net, have advanced segmentation precision through data augmentation and architecture optimization. However, challenges remain, including high computational demands and noise handling [5]. Research is focusing on integrating multiple models and optimizing preprocessing to address these issues, aiming for more robust and efficient methods suitable for diverse clinical settings. Additionally, advancements in heterogeneous system-on-chip (SoC) based simulations, such as the Lattice-Boltzmann interactive blood flow simulation pipeline [6] and the Lattice-Boltzmann visual simulation system [7], highlight strategies for optimizing processing speed and integrating specialized hardware. To provide a comprehensive overview of these developments, Table 1 summarizes key literature contributions, their methodologies, and performance metrics.

Table 1. Summary of related work

Authors	Methods used	Advantages	Limitations	Performance
Xu *et al.* 2019 [8]	LSTM-based multi-modal U-Net	Captures long-term dependencies; good for sequential MRI data	High computational complexity; potential overfitting	Dice score: 0.84, sensitivity: 0.81
Raza *et al.* 2023 [9]	dResU-Net (3D deep residual U-Net for MRI)	High segmentation accuracy; effective for multimodal MRI data	High computational requirements	Dice similarity score 0.87 for the (WT) 0.77 (CT), and 0.74 for (ET)
Das *et al.* 2021 [10]	Cascaded CNN	Good for 3D MRI; hierarchical processing improves feature capture	High memory usage; longer training times	Dice score: 0.87, specificity: 0.89
Rajbdad *et al.* 2018 [11]	Automated fiducial points detection	Reduces manual intervention; efficient for human body segmentation	Less effective on complex brain structures	Precision: 89%, recall: 88%
Vijay *et al.* 2023 [12]	Residual SPP-powered 3D U-Net	Improved feature extraction with spatial pyramid pooling; robust segmentation	Requires large-scale data for training	Dice score: 0.89, specificity: 95.2%, sensitivity: 93.8%
Yang *et al.* 2015 [13]	MRI texture analysis for glioblastoma classification	Discriminative features for survival prediction and molecular subtype analysis	Older method; lacks advanced deep learning techniques	Accuracy: 87%, accuracy: 82%
Montaha *et al.* 2023 [14]	U-Net for 3D MRI tumor segmentation	Efficient architecture for volumetric data	Requires preprocessing; limited scalability	Dice score: 0.90, sensitivity: 92%, specificity: 91%
Sangui *et al.* 2023 [15]	3D U-Net for brain tumor segmentation	Strong segmentation performance with enhanced spatial coherence	High computational cost	Dice score: 0.88, precision: 90%, recall: 87%
Soltaninejad *et al.* 2020 [16]	Multi-resolution encoder-decoder networks	High efficiency and scalability for multi-resolution segmentation tasks	Limited to specific MRI modalities	Dice score: 0.85 (WT), 0.82 (CT).
Isensee *et al.* 2020 [17]	nnU-Net for brain tumor segmentation	Self-configuring network; superior performance across diverse datasets	Computationally intensive; requires fine-tuning for specific tasks	Dice score: 0.91, sensitivity: 94.5%, specificity: 93%
Ali *et al.* 2020 [18]	Ensemble of 2D/3D U-Nets	Combines the strengths of both 2D and 3D models for segmentation	Complex training process; high computational demand	Dice score: 0.90 (WT), 0.85 (CT), 0.83 (ET).
Ren *et al.* 2017 [19]	Faster R-CNN	Real-time performance; effective object detection	Not specifically designed for medical segmentation	Accuracy: 93%, FPS: 7

Traditional methods such as thresholding, region growth, and watershed algorithms struggle to detect tumor boundaries and handle appearance variability. Machine learning techniques, such as neural networks and support vector machines (SVMs), improve accuracy while relying heavily on feature selection, which limits performance. Deep learning models also struggle with generalization across datasets and imaging conditions. While U-Net and its variants perform advanced segmentation tasks, there are still gaps in the integration of multi-modal data for comprehensive tumor characterization [20]. A long short-term memory (LSTM) multi-modal U-Net addresses temporal dependencies, but it requires additional optimization for 3D data. Furthermore, alignment across imaging modalities remains a challenge, which Vijay *et al.* [12] attempted to address with their symmetric non-rigid registration technique. However, more progress is required to develop an end-to-end brain tumor segmentation solution.

To address these challenges, this paper proposes a fully automated deep learning-based brain tumor segmentation technique that combines different encoder-decoder convolutional models [21]. Our approach integrates U-Net, InceptionResNetV2, and W-Net models which are recognized for their effectiveness in medical image segmentation. Additionally, our approach addresses the limitations of prior work by improving segmentation accuracy and ensures precise alignment and generalizability across different imaging modalities, making it a robust solution for real-world clinical applications.

2.   METHOD

The precise segmentation of glioma subregions from medical imaging data, crucial for treatment planning and disease monitoring. Gliomas exhibit diverse characteristics in size, shape, and location, posing challenges for accurate segmentation. Traditional methods to deep learning techniques have been explored, yet achieving accurate and consistent segmentation remains a challenge. The implementation aims to leverage hybrid filter,advanced convolutional neural networks (CNN) architectures such as U-Net, W-Net, and InceptioResNetV2 and novel optimization algorithm to develop an ensembleas given in Figure 1, aiming to improve segmentation accuracy. The main objectives of this study are as follows:

− Preprocessing: apply a hybrid bilateral mean filter, N4ITK bias field correction, and normalization to reduce noise and improve feature extraction and classification performance.
− Segmentation: use an ensemble model combining U-Net, InceptionResNetV2, and W-Net architectures for improved segmentation accuracy.
− Optimization: introduce a modified African vulture optimization algorithm (MAVOA) to optimize the model's loss function.
− Evaluation: compare metrics such as accuracy, sensitivity, specificity, and area under the receiver operating characteristic (ROC) curve (AUC) to assess performance.
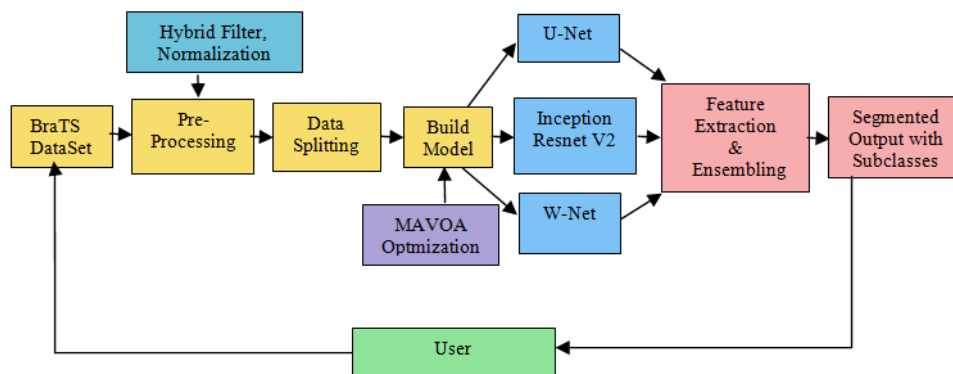

Figure 1. Architecture diagram

2.1. Data acquisition and preprocessing

The BraTS 2020 dataset is used for this study, consisting of multimodal MRI scans from glioma patients. These scans, collected from multiple institutions, have been standardized to ensure consistency. Each patient's data set includes four MRI modalities:

− T1-weighted (T1)
− Post-contrast T1-weighted (T1ce)
− T2-weighted (T2)
− Fluid attenuated inversion recovery (FLAIR)

These modalities provide distinct contrasts essential for accurate tumor segmentation by offering varied insights into tumor anatomy and pathology. The dataset includes expert-annotated labels for tumor sub-regions, crucial for training supervised learning models. The labels are provided as masks for each MRI slice, indicating pixel-wise classification of tumor sub-regions as follows:

− Necrotic and non-enhancing tumor core (NCR/NET): Label 1
− Peritumoral edema (ED): Label 2
− GD-enhancing tumor (ET): Label 3

To preprocess MRI images from the BraTS 2020 dataset, we performed a sequence of normalization followed by noise reduction using a hybrid bilateral mean filter given in Algorithm 1. In medical MRI image preprocessing, preserving edges while reducing noise is crucial for accurate diagnosis. The proposed filter enhances the quality of MRI images. The bilateral filter preserves edges by considering both spatial and intensity differences, while the mean filter reduces random noise. The proposed hybrid filtering algorithm leverages the edge-preserving capabilities of the bilateral filter and the noise-reducing properties of the mean filter. This combination is particularly effective for medical MRI images, where maintaining the integrity of anatomical structures is critical.

Algorithm 1. Hybrid bilateral mean filter

```
1    Input:          Original image I
2                    Bilateral filter parameters: σcolor and σspatial
3                    Mean filter window size: N
4    Output:         Hybrid filtered image Ihybrid
5    Procedure:  Bilateral Filtering:
6                    Apply bilateral filtering to the original image to produce a
     denoised version   Idenoised
7    Idenoised(i,j)=bilateral_filter(I,σcolor,σspatial)(i,j))
8                    Mean Filtering:
9                    Apply mean filtering to the original image to obtain a smoothed
     version Imean.
10
```

$$I_{mean}(i,j) = \frac{1}{N^2}\sum_{k=-N/2}^{N/2}\sum_{l=-N/2}^{N/2}(i+k,j+l)$$

```
11                  Hybrid Filtering:
12                  Combine the results of the bilateral filtering and the mean
     filtering
13   Ihybrid(i,j)=Idenoised(h,j)  +  (I(i,j)-Imean(i,j))
14   End
```

The hybrid bilateral mean filter is ideal for brain tumor segmentation as it preserves crucial tumor edges and reduces noise, enhancing segmentation accuracy. Despite its computational demands, it can be optimized for real-time use, making it valuable in clinical applications where precise and quick tumor detection is critical. The bilateral filter is well-suited for brain MRI scans because it can be fine-tuned to handle the subtle intensity differences between healthy tissue and tumor regions. By adjusting the σ_r parameter, the filter effectively reduces noise without losing critical tumor details. While it may not be ideal for impulse noise, it excels in managing the Gaussian or Rician noise typically found in MRI scans. Proper selection of σ_s and σ_r ensures optimal performance, enhancing the clarity and accuracy of brain tumor segmentation.

2.2. Tumor segmentation
2.2.1. U-Net architecture
U-Net is a CNN architecture optimized for high-resolution biomedical image segmentation [22]. It starts with an input layer for images of shape (IMG_SIZE,IMG_SIZE,2)(IMG_SIZE, IMG_SIZE, 2)(IMG_SIZE,IMG_SIZE,2), where IMG_SIZE denotes the spatial dimension and 2 represents the number of input channels. The encoder path uses two convolutional layers with rectified linear unit (ReLU) activations and He normal initialization, followed by max-pooling layers for down sampling. The architecture progresses through blocks with 32, 64, 128, 256, and 512 filters, with the fifth block including a dropout layer (rate 0.2). The bottleneck connects the encoder and decoder with two convolutional layers, each with 512 filters. In the decoder path, up sampling layers replace pooling to restore spatial dimensions, with each step followed by concatenation with corresponding encoder feature maps for precise localization. The decoder uses blocks with 256, 128, 64, and 32 filters, each containing two convolutional layers. The model concludes with a final convolutional layer (4 filters, 1×1 kernel) and a SoftMax activation to produce the segmentation map. The model is compiled using the categorical cross-entropy loss function and the MAVOA.

2.2.2. Inception Res-Net V2 architecture
InceptionResNetV2 is a sophisticated neural network architecture that combines Inception modules with residual connections to enhance image recognition efficiency and accuracy. In the proposed work the initial feature extraction occurs in the stem block, which includes convolutional and pooling layers to down sample the input. This block starts with three convolutional layers: 32 filters (3×3, stride 2, no padding), 32 filters (3×3, no padding), and 64 filters (3×3, padding), followed by a max-pooling layer (3×3 pool size, stride 2). It continues with a convolutional layer of 80 filters (1×1), another with 192 filters (3×3), and ends

with a max-pooling layer (3×3 pool size, stride 2). The core architecture features Inception-ResNet blocks. Inception-ResNet-A has parallel convolutional paths with various kernel sizes (1×1, 3×3, 5×5) and residual connections. The Reduction-A block reduces spatial dimensions using pooling and convolutional layers. Inception-ResNet-B follows, with more complex structures and residual connections, and Reduction-B further reduces dimensions. Inception-ResNet-C consists of intricate convolutional paths and residual connections. The network concludes with a global average pooling layer to reduce dimensions to 1×1, and a dense layer for final classification. InceptionResNetV2 effectively merges inception and residual methods, providing a powerful model for high-performance image recognition with efficient feature extraction.

2.2.3. W-Net architecture

W-Net is a deep learning architecture for image segmentation, especially effective for glioma sub region segmentation in MRI images. It features two stacked U-Nets, allowing for progressive refinement of segmentation results by using the output of the first U-Net as the input for the second. The first U-Net includes an encoder path with sequential convolutional and max-pooling layers, increasing the number of filters in each block (e.g., 32, 64, 128, 256), and a bottleneck layer to capture abstract features. The decoder path restores spatial dimensions using up sampling and convolutional layers, decreasing the number of filters (e.g., 256, 128, 64, 32). The output of the first U-Net is passed to the second U-Net, which has a similar structure. The second U-Net refines the segmentation map with its own encoder and decoder paths, again employing convolutional, max-pooling, and up sampling layers. The final output layer has filters matching the number of segmentation classes, followed by a soft max activation for multi-class segmentation. W-Net is compiled with loss functions like categorical cross-entropy, the MAVOA optimizer.

2.2.4. Ensemble model

The ensemble model integrates individual models, such as U-Net, InceptionResNetV2, and W-Net, each providing segmentation predictions for MRI images. In this approach [23], the predictions from these models are combined using an average weighting technique. For each pixel in the final segmentation map, the predicted probabilities from U-Net, InceptionResNetV2, and W-Net are averaged. By leveraging the strengths of these diverse models, the ensemble method enhances the accuracy and robustness of glioma subregion segmentation, offering more detailed and precise results than any single model could achieve alone. Table 2 shows the hyperparameters that are employed in the segmentation model.

Table 2. Details of hyperparameters

Hyperparameters	Details
Epochs	100
Batch size	16
Learning rate	0.001
Dilation rate	3
Dropout rate	0.2

2.3. Modified African vulture optimization algorithm

Nature-inspired optimization algorithms enhance deep learning in medical image analysis by efficiently navigating complex data, improving diagnosis and treatment planning. In this aspect we proposed a novel MAVOA algorithm, given in Algorithm 2 for image segmentation incorporates spatial awareness, localized foraging, and adaptive mutation, enhancing its effectiveness for segmenting objects from images with improved accuracy and spatial coherence.

Algorithm 2. Modified African vulture optimization algorithm for image segmentation

```
1    Input: Image I, Number of vultures N, Maximum iterations T, Parameters α,β
2    Output: Optimized segmentation S*
3    Initialization:
4         Randomly initialize vultures' positions within the image space:
5    InitializeVultures(N,I)
6         Initialize best solution found so far:
7    best_solution=None, best_fitness=∞
8    Main Loop:
9         for t=1 to T do:
10             Evaluate fitness for each vulture :EvaluateFitness(I,vultures)
11             Update vultures' positions:
12    UpdateVulturesPosition(I,vultures,best_solution)
13             Select the best solution found so far:
             current_best_solution,current_best_fitness=SelectBestSolution(vultures)
```

```
14                        if current_best_fitness<best_fitness then:
15
16      best_solution=current_best_solution,best_fitness=current_best_fitness
17                   if stopping criterion met then:
18                              break
19      Update Vultures' Positions:
20      UpdateVulturesPosition(I,vultures,best_solution)
21                   for each vulture v do:
22                        Update vulture's position based on attraction and social
23      components:
24      update_vulture_position(I,v,best_solution)
25      Fitness Evaluation:
26      EvaluateFitness(I,vultures)
27                   for each vulture v do:
28                        Calculate fitness based on segmentation accuracy and spatial
29      coherence:
30      v.fitness=calculate_fitness (I,v.position)
31       Utility Functions:
32      sum_of_other_vultures_influence(v,best_solution)
33                        Calculate the sum of other vultures' influence on a vulture's
34      position.
35                   Other utility functions (not explicitly shown) for initializing
36      vultures, selecting
                     the best solution, and stopping criterion.
        Fitness Calculation:
                 calculate_fitness(I,segmentation)calculate_fitness(I,segmentation):
                    Compute segmentation accuracy and spatial coherence.
                    Combine accuracy and coherence into a single fitness value.
```

The AVOA for medical image segmentation is enhanced by including spatial awareness in the fitness calculation, which penalizes incoherent solutions. Vultures' movements now incorporate a localized foraging strategy and a dynamic exploration radius based on image context. Adaptive mutation adjusts strength and probability based on optimization progress. The fitness function also considers multiple objectives, such as segmentation accuracy and spatial coherence, to ensure precise results.

3. RESULTS AND DISCUSSION

The ensemble model generated a final segmentation map for the input MRI images by averaging predictions from U-Net, InceptionResNetV2, and W-Net. This combined approach is visualized in Figure 2, where each pixel in the segmentation map reflects the aggregated confidence of the models regarding the presence of various glioma subregions.
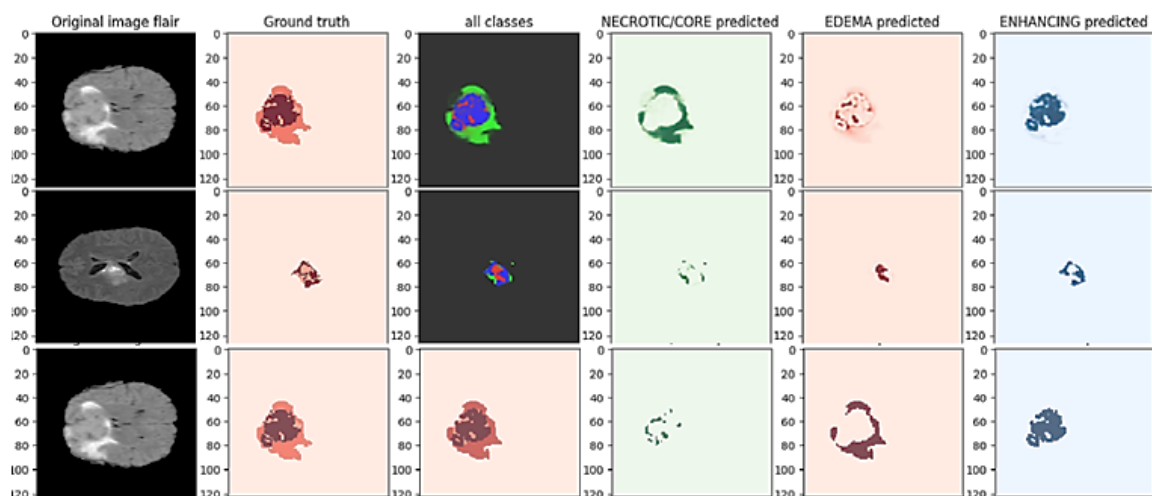

Figure 2. Glioma sub region segmentation of ensemble mode

To enhance segmentation accuracy, optional post-processing steps such as thresholding, morphological operations, or connected component analysis may be applied to the ensemble output. The performance metrics for the ensemble model are as follows: accuracy of 98.2%, loss of 0.023, recall of 0.982, mean intersection over union (IOU) of 0.972, dice coefficient of 0.96, precision of 0.991, sensitivity of 0.98, and specificity of 0.981. The dice coefficients for specific glioma subregions were 0.96 for necrotic regions, 0.970 for edema, and 0.91 for enhancing regions. These metrics provide a detailed evaluation of the model's effectiveness and highlight areas for potential optimization. Figure 3 displays the training and validation plots for accuracy, loss, dice coefficient, and mean IOU.
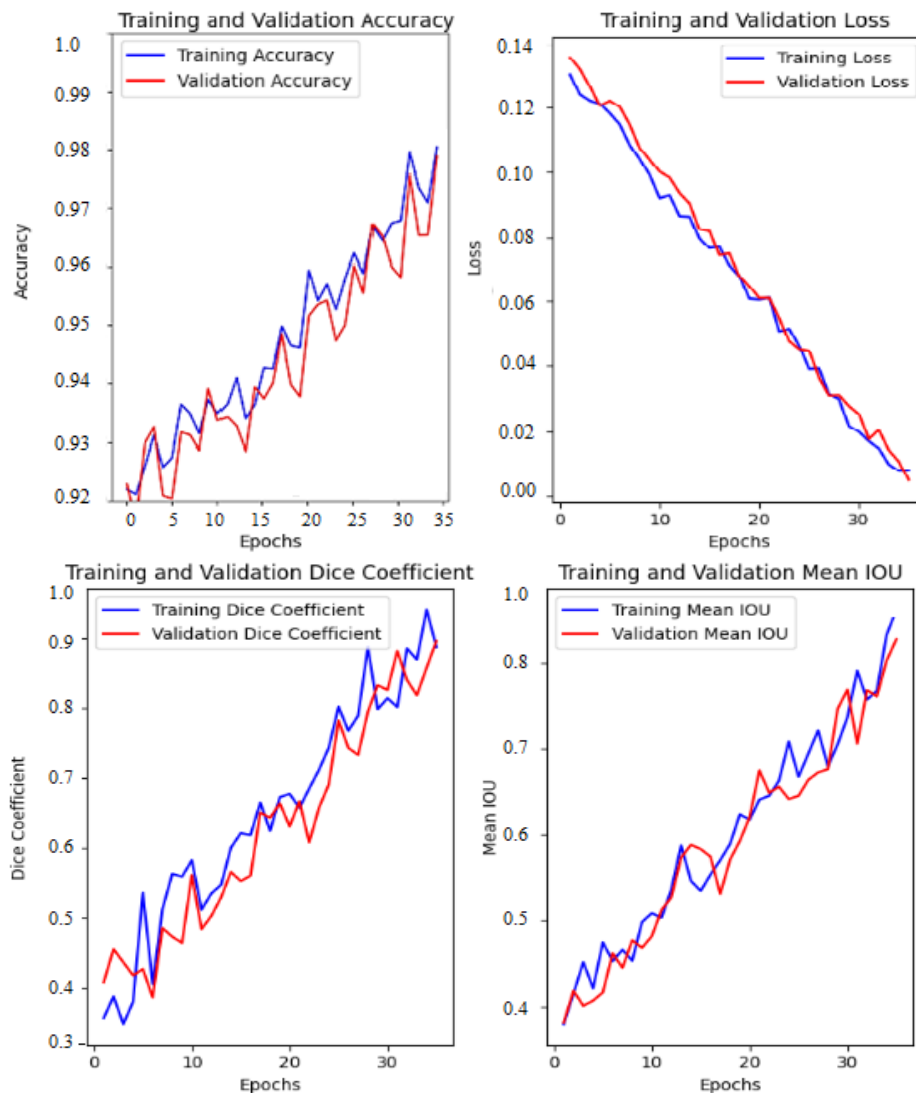
Figure 3. Graphical representation of accuracy, loss, dice coefficient, and mean IOU of the ensembling model

Additionally, Figure 4 presents a comparative analysis of metrics including recall, specificity, sensitivity, and precision, contrasting the ensemble model's performance with that of region convolutional neural network (RCNN), U-Net, and W-Net combined with a decision tree. This comparison underscores the ensemble model's superior performance in segmentation tasks. Our brain tumor segmentation implementation can benefit from insights into real-time performance demonstrated by Lattice-Boltzmann simulation methods [24]. The interactive blood flow simulation highlights strategies for optimizing processing speed, while the SoC-based system underscores the advantages of specialized hardware. Adapting these insights could enhance the efficiency and real-time capabilities of our segmentation approach [25].
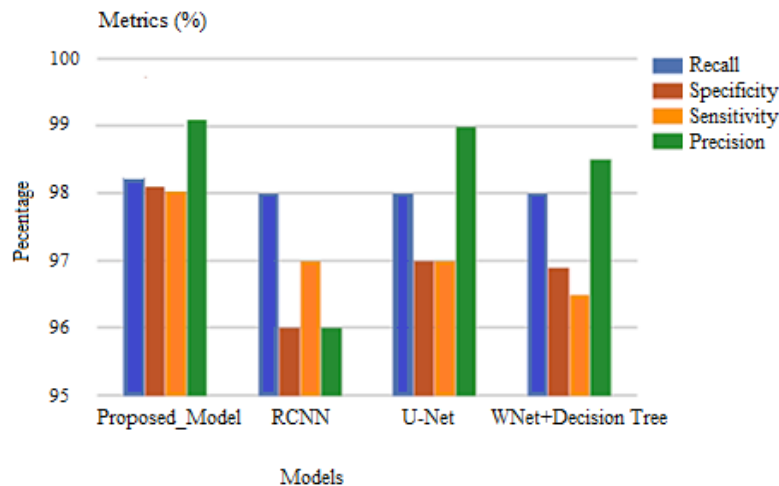
Figure 4. Comparison of metrics (recall, specificity, sensitivity, and precision) with other models

4. CONCLUSION

This study presents a novel approach for accurate glioma subregion segmentation from MRI data, integrating a hybrid bilateral mean filter for preprocessing with an ensemble model comprising U-Net, InceptionV2, InceptionResNetV2, and W-Net architectures. Additionally, the introduction of a MAVOA has led to impressive performance metrics on BraTS 2020 data, with a loss of 0.023 and high accuracy 98.2%, recall 98.2%, mean IOU 97.2%, dice coefficient 0.96, precision of 99.1%, sensitivity of 98%, and specificity of 98.1%. The model effectively delineates glioma subregions, achieving dice coefficients of 0.96 for necrotic areas, 0.97 for edema, and 0.91 for enhancing regions. On the BraTS 2021 dataset, the model maintained high accuracy of 96.4%, mean IOU 95.9%, and dice coefficients of 0.91 for necrotic areas, 0.95 for edema, and 0.92 for enhancing regions. These findings demonstrate a significant advancement in the precision and effectiveness of glioma segmentation, which can greatly impact clinical practice by enhancing diagnosis, treatment planning, and disease monitoring. Future research should concentrate on clinical validation, improving model generalizability, and improving interpretability through explainable artificial intelligent (AI). Exploring new imaging modalities and incorporating the model into clinical systems could help to advance neurooncology and patient care.

REFERENCES

[1] K. K. Farmanfarma, M. Mohammadian, Z. Shahabinia, S. Hassanipour, and E. Salehiniya, "Brain cancer in the world: an epidemiological review," *World Cancer Research Journal*, vol. 6, 2019, doi: 10.32113/wcrj_20197_1356.

[2] S. Das, "Brain tumor segmentation from mri images using deep learning framework," in *Advances in Intelligent Systems and Computing*, vol. 1119, 2020, pp. 105–114, doi: 10.1007/978-981-15-2414-1_11.

[3] D. N. Louis *et al.*, "The 2016 world health organization classification of tumors of the central nervous system: a summary," *Acta Neuropathologica*, vol. 131, no. 6, pp. 803–820, Jun. 2016, doi: 10.1007/s00401-016-1545-1.

[4] H. Dong, G. Yang, F. Liu, Y. Mo, and Y. Guo, "Automatic brain tumor detection and segmentation using u-net based fully convolutional networks," in *Communications in Computer and Information Science*, vol. 723, 2017, pp. 506–517, doi: 10.1007/978-3-319-60964-5_44.

[5] K. Bhagyalaxmi, B. Dwarakanath, and P. V. P. Reddy, "Deep learning for multi-grade brain tumor detection and classification: a prospective survey," *Multimedia Tools and Applications*, vol. 83, no. 25, pp. 65889–65911, Jan. 2024, doi: 10.1007/s11042-024-18129-8.

[6] S. Mohanty and S. P. Dakua, "Toward computing cross-modality symmetric non-rigid medical image registration," *IEEE Access*, vol. 10, pp. 24528–24539, 2022, doi: 10.1109/ACCESS.2022.3154771.

[7] Y. Regaya, A. Amira, and S. P. Dakua, "Development of a cerebral aneurysm segmentation method to prevent sentinel hemorrhage," *Network Modeling Analysis in Health Informatics and Bioinformatics*, vol. 12, no. 1, p. 18, Mar. 2023, doi: 10.1007/s13721-023-00412-7.

[8] F. Xu, H. Ma, J. Sun, R. Wu, X. Liu, and Y. Kong, "LSTM-based multi-modal unet for brain tumor segmentation," in *2019 IEEE 4th International Conference on Image, Vision and Computing (ICIVC)*, IEEE, Jul. 2019, pp. 236–240, doi: 10.1109/ICIVC47709.2019.8981027.

[9] R. Raza, U. I. Bajwa, Y. Mehmood, M. W. Anwar, and M. H. Jamal, "dResU-Net: 3D deep residual U-Net based brain tumor

segmentation from multimodal MRI," *Biomedical Signal Processing and Control,* vol. 79, p. 103861, 2023, doi: 10.1016/j.bspc.2022.103861.

[10] S. Das, M. K. Swain, G. K. Nayak, and S. Saxena, "Brain tumor segmentation from 3d mri slices using cascading convolutional neural networks," in *International Conference on Emerging Trends and Advances in Electrical Engineering and Renewable Energy*, 2021, vol. 709, pp. 119–126, doi: 10.1007/978-981-15-8752-8_12.

[11] F. Rajbdad, M. Aslam, S. Azmat, T. Ali, and S. Khattak, "Automated fiducial points detection using human body segmentation," *Arabian Journal for Science and Engineering*, vol. 43, no. 2, pp. 509–524, Feb. 2018, doi: 10.1007/s13369-017-2646-4.

[12] S. Vijay, T. Guhan, K. Srinivasan, P. D. R. Vincent, and C. Y. Chang, "MRI brain tumor segmentation using residual Spatial Pyramid Pooling-powered 3D U-Net," *Fronties in Public Health*, vol. 11, p. 1091850, 2023, doi: 10.3389/fpubh.2023.1091850.

[13] D. Yang, G. Rao, J. Martinez, A. Veeraraghavan, and A. Rao, "Evaluation of tumor-derived MRI-texture features for discrimination of molecular subtypes and prediction of 12-month survival status in glioblastoma," *Medical Physics*, vol. 42, no. 7, pp. 4328-4338, Jul. 2015, doi: 10.1118/1.4934373.

[14] S. Montaha, S. Azam, A. K. M. R. H. Rafid, Md. Z. Hasan, and A. Karim, "Brain Tumor Segmentation from 3D MRI Scans Using U-Net," *SN Computer Science*, vol. 4, no. 386, 2023, doi: 10.1007/s42979-023-01854-6.

[15] S. Sangui, T. Iqbal, P. C. Chandra, S. Kr Ghosh, and A. Ghosh, "3D MRI Segmentation using U-Net Architecture for the detection of Brain Tumor," *Procedia Computer Science*, vol. 218, pp. 542-553, 2023, doi: 10.1016/j.procs.2023.01.036.

[16] M. Soltaninejad, T. Pridmore, and M. Pound, "Efficient MRI Brain Tumor Segmentation Using Multi-Resolution Encoder-Decoder Networks," in *Brainlesion: Glioma, Multiple Sclerosis, Stroke and Traumatic Brain Injuries: 6th International Workshop, BrainLes 2020, Held in Conjunction with MICCAI 2020,* Lima, Peru, Springer International Publishing, October 4, 2020, pp. 31-39, doi: 10.1007/978-3-030-72087-2_3.

[17] F. Isensee, P. F. J¨ager, P. M. Full, P. Vollmuth, and K. H. Maier-Hein, "nnU-Net for Brain Tumor Segmentation," *arXiv*, 2020, doi: 10.48550/arXiv.2011.00848.

[18] M. J. Ali, M. T. Akram, H. Saleem, B. Raza, and A. R. Shahid, "Glioma Segmentation Using Ensemble of 2D/3D U-Nets and Survival Prediction Using Multiple Features Fusion," *Brainlesion: Glioma, Multiple Sclerosis, Stroke and Traumatic Brain Injuries: 6th International Workshop, BrainLes 2020, Held in Conjunction with MICCAI 2020,* Lima, Peru, Springer International Publishing, 2020, vol. 12659, doi: 10.1007/978-3-030-72087-2_17.

[19] S. Ren, K. He, R. Girshick, and J. Sun, "Faster r-cnn: towards real-time object detection with region proposal networks," *IEEE Transactions on Pattern Analysis and Machine Intelligence*, vol. 39, no. 6, pp. 1137–1149, Jun. 2017, doi: 10.1109/TPAMI.2016.2577031.

[20] S. Das, M. ku Swain, G. K. Nayak, S. Saxena, and S. C. Satpathy, "Effect of learning parameters on the performance of u-net model in segmentation of brain tumor," *Multimedia Tools and Applications*, vol. 81, no. 24, pp. 34717–34735, Oct. 2022, doi: 10.1007/s11042-021-11273-5.

[21] K. Bhagyalaxmi, B. Dwarakanath, and P. V. Reddy, "Ensemble of deep learning models and machine learning classifiers for the classification of brain tumors," in *2024 2nd International Conference on Computer, Communication and Control (IC4)*, IEEE, Feb. 2024, pp. 1–6, doi: 10.1109/IC457434.2024.10486611.

[22] N. S. Punn and S. Agarwal, "Modality specific U-Net variants for biomedical image segmentation: a survey," *Artificial Intelligence Review*, vol. 55, pp. 5845–5889, 2022, doi: 10.1007/s10462-022-10152-1.

[23] T. Vaiyapuri, J. Mahalingam, S. Ahmad, H. A. M. Abdeljaber, E. Yang, and S. -Y. Jeong, "Ensemble Learning Driven Computer-Aided Diagnosis Model for Brain Tumor Classification on Magnetic Resonance Imaging," in *IEEE Access*, vol. 11, pp. 91398-91406, 2023, doi: 10.1109/ACCESS.2023.3306961.

[24] S. S. Esfahani *et al.*, "Lattice-boltzmann interactive blood flow simulation pipeline," *International Journal of Computer Assisted Radiology and Surgery*, vol. 15, no. 4, pp. 629–639, Apr. 2020, doi: 10.1007/s11548-020-02120-3.

[25] X. Zhai *et al.*, "Heterogeneous system-on-chip-based lattice-boltzmann visual simulation system," *IEEE Systems Journal*, vol. 14, no. 2, pp. 1592–1601, Jun. 2020, doi: 10.1109/JSYST.2019.2952459.

BIOGRAPHIES OF AUTHORS

Bhagyalaxmi Kuntiyellannagari 🆔 g⁺ SC ⊙ is a research scholar at Department of Computer Science and Engineering, SRMIST Ramapuram, Chennai, India. She is M.Tech. (CSE) from JNTU having 20 years teaching experience. Published around 20 papers in international journals and conferences. Her interest areas are deep learning and image processing. She is a member of CSI and ISTE. She can be contacted at email: bk8019@srmist.edu.in.

Dr. Bhoopalan Dwarakanath M.Tech, Ph.D. 🆔 g⁺ SC ⊙ is Associate Professor in the Department of Information Technology, SRMIST, Ramapuram, Chennai, Tamil Nadu. Ph.D., in machine learning - information technology in 2019 from Hindustan Institute of Technology and Science, Chennai, Tamil Nadu. He has done his M.Tech., CSE from Vellore Institute of Technology, Vellore in the year 2004. He has 30 publications in International Journals and Conferences. His research interests include machine learning, image processing, and network programming. He is an active member of ACM, IET, ISTE, CSI, and IEANG. He can be contacted at email: dwarakab@srmist.edu.in.